applied sciences

MDPI

Article

Optimizing the Control Level Factors of an Ultrasonic Plastic Welding Machine Affecting the Durability of the Knots of Trawl Nets Using the Taguchi Experimental Method

Nghia-Danh Nguyen [1,2] and Shyh-Chour Huang [1,*]

[1] Department of Mechanical Engineering, National Kaohsiung University of Science and Technology, Kaohsiung 807618, Taiwan; i111142109@nkust.edu.tw

[2] Faculty of Engineering and Technology, Nguyen Tat Thanh University, 300a Nguyen Tat Thanh, Ward 13, District 4, Ho Chi Minh City 70000, Vietnam

* Correspondence: shuang@nkust.edu.tw

Abstract: Ultrasonic welding is a high-frequency method of welding that uses mechanical energy to generate heat. This is a clean welding method and very suitable for plastic welding. In this study, using the Taguchi experimental method, the control factors of an ultrasonic plastic welding machine were optimized to affect the durability of knots of trawl nets made from polyamide (PA) and polypropylene (PP) filaments as an alternative to the traditional mesh knitting method. After optimization, the PA knots had an amplitude of 32 µm (34%), a welding pressure of 2.5 kg/cm^2 (41%), a hold time of 0.35 s (24%), and a speed of 5.5 mm/s (1%). The knots made of PP filament had relatively stable strength after optimization, with an amplitude of 36 µm (25%), a welding pressure of 2.0 kg/cm^2 (22%), a hold time of 0.25 s (16%), and a speed of 6.0 mm/s (37%). Finally, validation experiments were conducted to verify the results obtained in this study.

Keywords: polyamide; polypropylene; tensile strength; experiment method; knots of trawl; ultrasonic plastic welding

check for updates

Citation: Nguyen, N.-D.; Huang, S.-C. Optimizing the Control Level Factors of an Ultrasonic Plastic Welding Machine Affecting the Durability of the Knots of Trawl Nets Using the Taguchi Experimental Method. *Appl. Sci.* **2023**, *13*, 9061. https://doi.org/10.3390/app13169061

Academic Editor: Jacek Tomków

Received: 18 July 2023
Revised: 1 August 2023
Accepted: 7 August 2023
Published: 8 August 2023

1. Introduction

Trawl net [1] is a type of net that is strung or pulled in an aquatic environment to catch fish. Currently, together with the Raschel net [2], they are also used to make net cages, and thus used in passive fishing. In this method, the net cages are arranged in an open space along the river or the coast, which makes it rather advantageous; for example, the water source in the cage is always renewed, it is easier than offshore fishing methods, and it also minimizes the risk of common diseases than methods involving aquatic products in pond and lake environments. The net cages are arranged in an open space; hence, they are also directly affected by environmental factors such as floods and storms that put a stress on seafood. With these advantages, the fishery output exploited using this method can be up to 75 tons of products (accounting for nearly 50% of the world's fishery production) by 2040 [3]. In recent years, many studies relating to net cages have been conducted; for example, Hao Chen et al. [4] built a numerical model based on the aggregate block structure model and the digital porous environment model to analyze the fluid–structure interaction of the flow through and around aquaculture net cages. They found that the mesh strain yielded good results in the middle part, while the bottom part had a large displacement compared to the experimental results. Biao Su et al. [5] integrated acoustic positioning sensor data for real-time monitoring of mesh cage deformations and observed that the proposed method was highly effective, but it was necessary to use additional depth sensors, IMUs, or a 3D interpolation algorithm to achieve better accuracy. Paweł Baranowski et al. [6] developed a numerical method to evaluate the interaction of 3D objects with polypropylene meshes. They found that the lattice configuration affects the object in different ways, reducing the speed and changing the trajectory of the 3D object. Overall, these studies have digitized the interaction of water flow on the net cage structure, rendering the control of the capture and aquaculture process more efficient. However, due to many reasons, such as environment, water flow, or inappropriate selection of nets, the phenomenon of net tearing causing loss of fishery production still occurs [7].

This study relates to the ultrasonic welding [8] method of bonding of two objects through the generation of heat from high-frequency oscillations; it is a clean method and is very suitable for application to products related to plastic. To have a good weld point, the Taguchi method (a statistical method developed by Genichi Taguchi to improve the quality of manufactured goods) is often applied to optimize the factor variables. In recent years, many researchers have used this method. Chil-Chyuan et al. [9] used the Taguchi method to study the effects of welding factors on the strength of ultrasonic welds and observed that amplitude was the most important parameter of the ultrasonic plastic welding machine, accounting for 62% of the weld quality. This method has been widely applied in engineering and biotechnology. Mahmoudian et al. [10] performed methyl-methacrylate polymerization to improve the reciprocation of nanoparticles, and Costa et al. [11] optimized the process factors of the steel turning process using the Taguchi method. Bo-Lin Jian et al. [12] optimized the cutting parameters for precision lathes via the Taguchi method. Their study showed that the cutting depth and spindle speed have the greatest impact, and directly affected the surface roughness of the product and the material removal rate. Son et al. [13] used the Taguchi method and optimized the control factors of the automatic net-wrapper robot arm. Their study determined the appropriate suction pressure for the ideal cake state for commercialization without destroying the relatively brittle structure like a net wrapper.

In this study, an ultrasonic plastic welding machine (UPWM) [14] was used to create new knots of trawl and raschel nets to replace the traditional knitting method. For this, it was essential to optimize the control factors of the UPWM machine. Using the earlier published method [15], the tensile strength of knots made using the UPWM was tested at different levels and factors on the tensile tester machine (TTM). Then, the three most promising levels of factors are selected for optimization using the Taguchi method to find the parameter set providing the highest efficiency to the tensile strength of the knot. Finally, validation experiments were performed to verify the optimal set of parameters obtained in this study.

This paper is structured as follows: the experimental procedure is presented after the introduction. Then, the results are discussed, followed by a conclusion.

2. Materials and Methods

2.1. Materials and Equipment

The trawl net is knitted using polyamide (PA) filament; at the position of grid formation, two PA ropes are knitted together manually (Figure 1a) [16]. The net has a square or diamond shape, depending on the purpose of use, but the fisherman uses the appropriate wire cross-section. Unlike trawl nets, raschel nets are made from polypropylene fibers, which comprise 8–16 smaller fibers [17], and thus are stronger than PA ropes. However, to shape the raschel grid, part of the wire cross-section is interlocked (Figure 1b); hence, the knot position is relatively weak compared to the original wire.

In this study, the knot strength of the trawl net and raschel net made from PA and PP fibers, respectively, created using a UPWM were compared to that prepared with the original material. To obtain the tensile strength graph of PA and PP filaments, a tensile tester machine (FT plus, Ametek Inc., East Hampshire, England) together with Nexygen Plus Software (version 3.0.0.1) was used. Here, two samples of PA and PP wires with a cross-section of 0.4 mm and a length of 2.5 cm (Figure 2a) were clamp fixed at both ends of the wire and an extensometer link (Figure 2b) was established with a speed of 5 mm/min. The value obtained from the loadcell was converted to the tensile strength value using Equations (1) and (2) [18]. The operation principle of the tensile tester machine is roughly presented in Figure 2c. Here, inside the load cell, the Wheatstone bridge is made up of four rheostats, with an output voltage of approximately 0 V being sent to the processor board. For tensile loads, the voltage is set to increase up to +10 V (about 1000 N ± 0.5%) and conversely decreased to −10 V for compressive loads. The voltage values are converted to 16-bit data using a capacitor-based analog-to-digital converter. For the extensometer, the slider movement is measured by directly counting the pulses generated via a high-resolution digital encoder controlled with the lead screw. The phase generated via the encoder is important to ensure correct rise or fall of the lead screw.

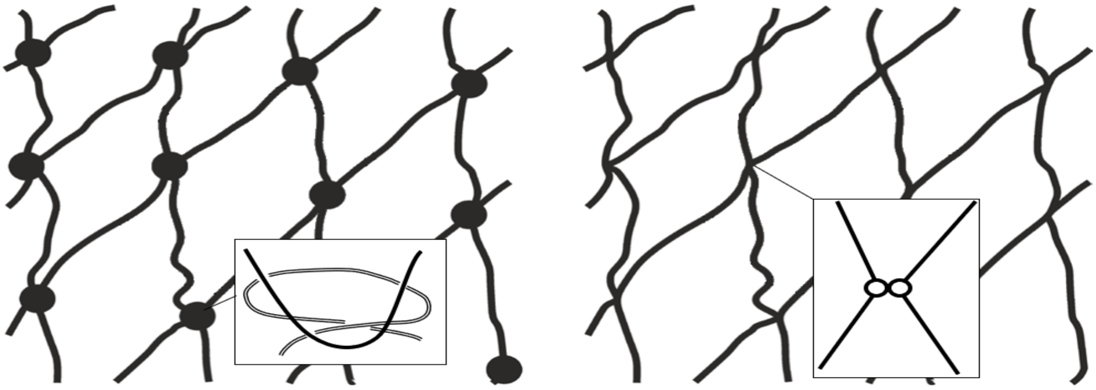

(a) (b)

Figure 1. The shape structure of the trawl nets and raschel nets. (**a**) Trawl nets; (**b**) Raschel nets.

$$\sigma_T = \frac{F}{A} \tag{1}$$

$$\varepsilon_T = \frac{\Delta L_0}{L_0} \tag{2}$$

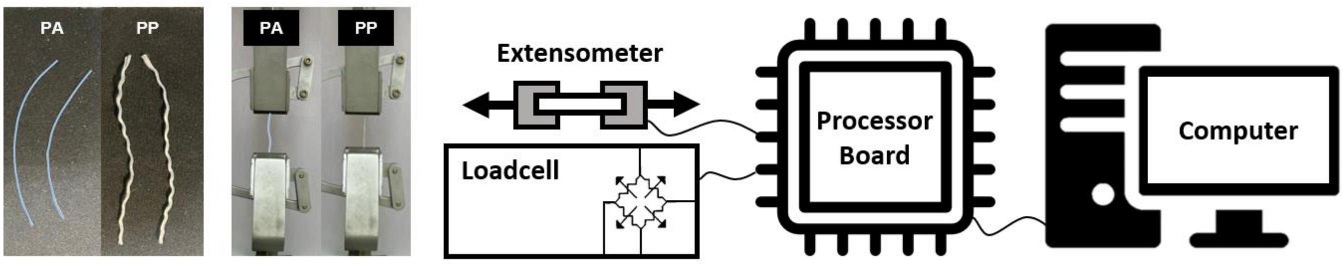

(a) (b) (c)

Figure 2. Schematic diagram of loadcell and extensometer sensing system. (**a**) PA and PP filaments; (**b**) tensile tester of materials; (**c**) system operation diagram.

In Equation (1), F is the measured force concerned (N), A is the initial cross-sectional area of the specimen (mm^2). In Equation (2), L_0 is the initial length (mm) and L_1 is determined as the end length (mm).

Figure 3 shows that the PA filament has a maximum stress value of up to 120 Mpa, with more brittle mechanical properties (strain 0.16) than that of the PP filament with a stress value of 142 Mpa (strain 0.38). The stress results of the two types are somewhat larger and the mechanical properties are somewhat more brittle than that of the standard PA and PP filaments [19,20] due to the wire structure being different from the standard stress test form (dog-bone specimen) and alteration in the chemical composition inside the material from the manufacturer to suit the needs of users.

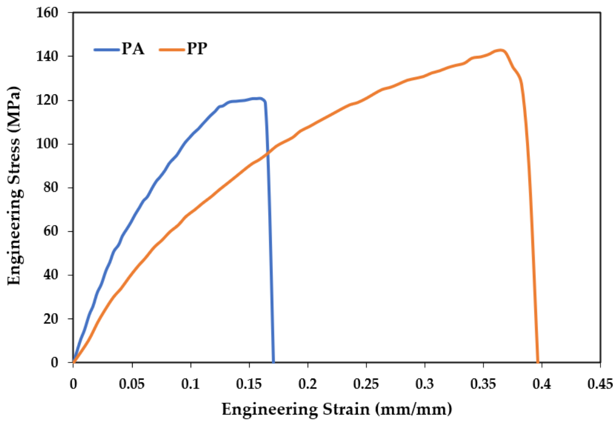

Figure 3. The tensile strength of polyamide (PA) and polypropylene (PP) filaments.

The UPWM device (Linggao K745, LINGKE Inc., Zhuhai City, China) used in this study has an ultrasonic frequency of 35 kHz, a power of 900 W with an amplitude up to 40 µm (Figure 4a). With an input of 220 V/60 Hz power supply, the generator was responsible for amplifying the value into ultrasonic energy with a frequency of 35 kHz. From the ultrasonic energy source, the high-frequency electrical energy was converted into high-frequency mechanical motion through the converter and was allowed to pass through the booster to increase the amplitude by 1:2 before reaching the plastic part, with the output diameter of the horn (Figure 4a) being 1.2 mm (Figure 4b). The material was fixed on the trigger (Figure 4c). Figure 4d shows the process before and after welding the knot with UPWM. Unlike Auxetic materials, which have elastic properties of negative Poisson's ratio (NPR) [21,22], in UPWM machining, when subjected to the vertical pressure of the horn and the trigger, the material tends to change form horizontally and link two objects together through high-frequency mechanical motion [23], so the size of the weld tends to increase in the horizontal direction.

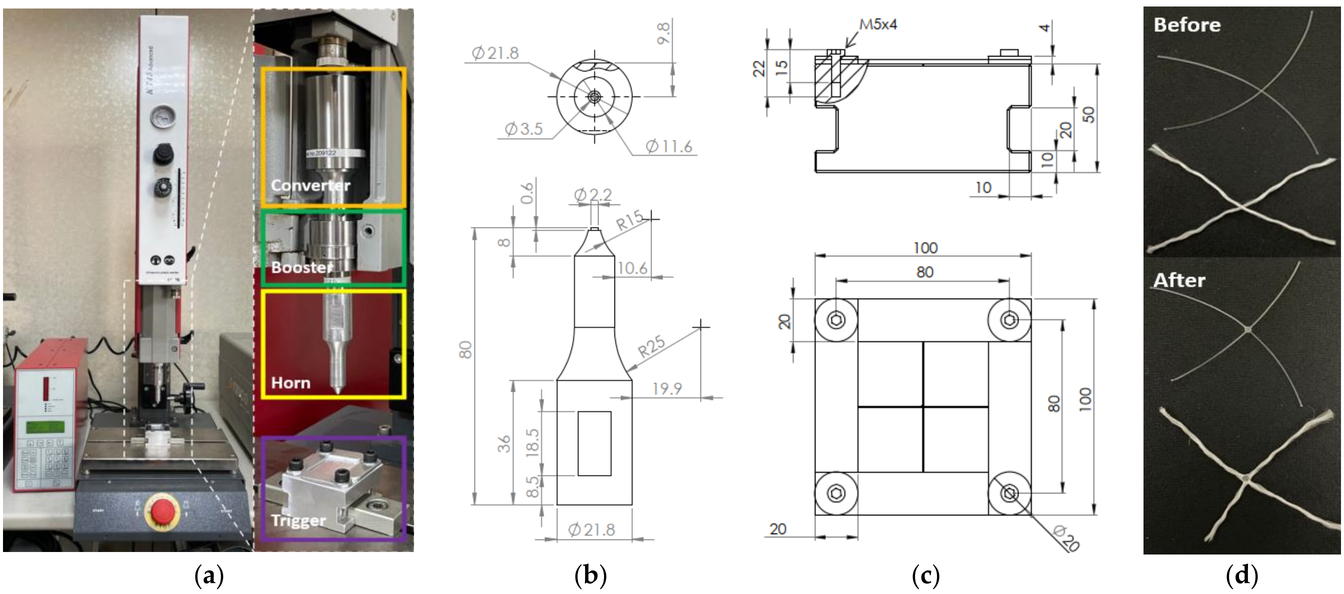

Figure 4. Preparation of polyamide (PA) and polypropylene (PP) knots with ultrasonic plastic welding machine (UPWM). (**a**) UPWM model Linggao K745; (**b**) horn; (**c**) trigger; (**d**) PA and PP knots.

2.2. Experiment Details

Figure 5 shows the experimental procedure of this study. A total of 360 samples at nine levels of four factors (amplitude, weld pressure, speed, and hold time) [24] for PA and PP knots were performed on the UPWM for a trial-and-error period. The levels of the factors used for the experiments are shown in Table 1. In there, one factor considered changes the level from 1 to 9, while the remaining factors have a fixed value. Two values of the knots were considered, thickness (digimatic micrometer of Mitutoyo) and tensile strength (TTM), respectively, on the interval plot [25] to search for three optimal levels corresponding to the factors. Continuously, with four factors and three levels selected, 54 samples were performed, amounting to 18 experiments (L9 and repeat 3) for both PA and PP. The larger-the-better of Taguchi method was applied to optimize the levels of control factors that directly affect the strength of the weld. Finally, the optimized parameter set along with three non-optimized parameter sets were selected to apply to 20 samples (Table 1). Testing of the samples on TTM were continued for durability to verify the effectiveness of this research.

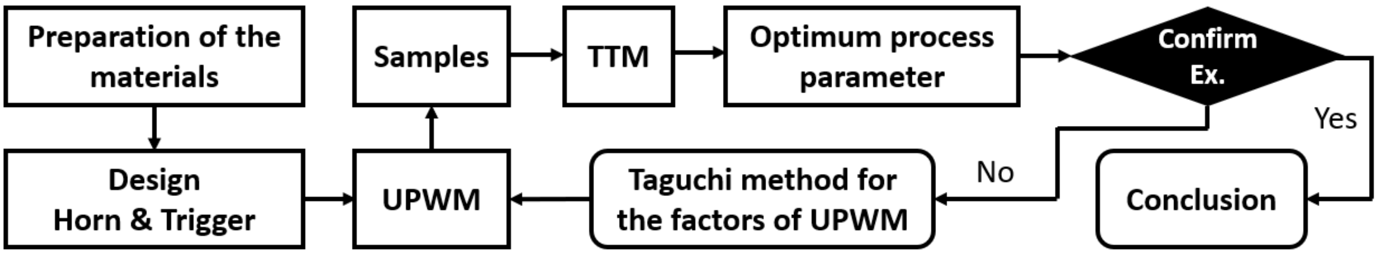

Figure 5. The process of the experiment.

Table 1. Specification use for the ultrasonic plastic welding machine (UPWM).

Amplitude (60–100) [%]	Weld Pressure (2.0–6.0) [kg/cm^2]	Hold Time (0.1–0.5) [s]	Speed (3.0–7.0) [mm/s]
80	3.0	0.3	5.0

3. Results and Discussion

3.1. Polyamide

Figure 6 shows the interval plots for the thickness and strength of polyamide welds at levels of control factors. Considering the amplitude factor (Figure 6a), the histogram shows amplitude levels varying from 24 µm to 40 µm (60% to 100%) when the other factors were fixed (Table 1). According to the results, the method could not be performed on plastic fibers at 60%, and the value of weld strength is not much different at the remaining amplitude levels. In addition, the thickness of the weld fluctuated in the range of 0.05 mm to 0.07 mm and provided the best results at 5 (80%—32 µm) with a weld strength and thickness of 70 Mpa and 0.065 mm, respectively. Considering the weld pressure factor (Figure 6b), the welding pressure levels varied from 2.0 kg/cm^2 to 6.0 kg/cm^2. When the welding pressure increased, the thickness of the weld tended to decrease, which partly reduced the durability of weld. For this factor, when the weld strength value did not change much, the thickness of the weld was considered at level 2 (2.5 kg/cm^2) for the most optimal value. In terms of the hold time factor (Figure 6c), the histogram in this figure shows varying hold time levels from 0.1 s to 0.5 s, while the other factors were fixed. In general, changing the hold time did not affect the strength of the weld much. Similar to the previous factor, at the hold time factor, the weld strength value at level 7 (0.4 s) provided the best results but still ensured its thickness. The mean thickness of the knots seems to be lower than the expected (about 0.07 mm) at level 3 (0.2 s). This may be due to the fact that the mechanical properties of the plastic fibers chosen for the test were not uniform with the rest of the test pieces. In order for the experimental results to be objective, this noise signal is still kept. For the speed factor (Figure 6d), the graph shows that the levels of the speed factor varied from 3.0 mm/s to 7.0 mm/s. When the speed increased, the thickness and weld strength tended to increase markedly. However, if the thickness of the weld is larger, the strength of the weld will decrease (levels 8 and 9). Therefore, the best results were achieved at level 7 (6 mm/s) with an average weld strength of 68 Mpa and a thickness of 0.17 mm. The best three levels of control factors were selected and they are presented in Table 2.

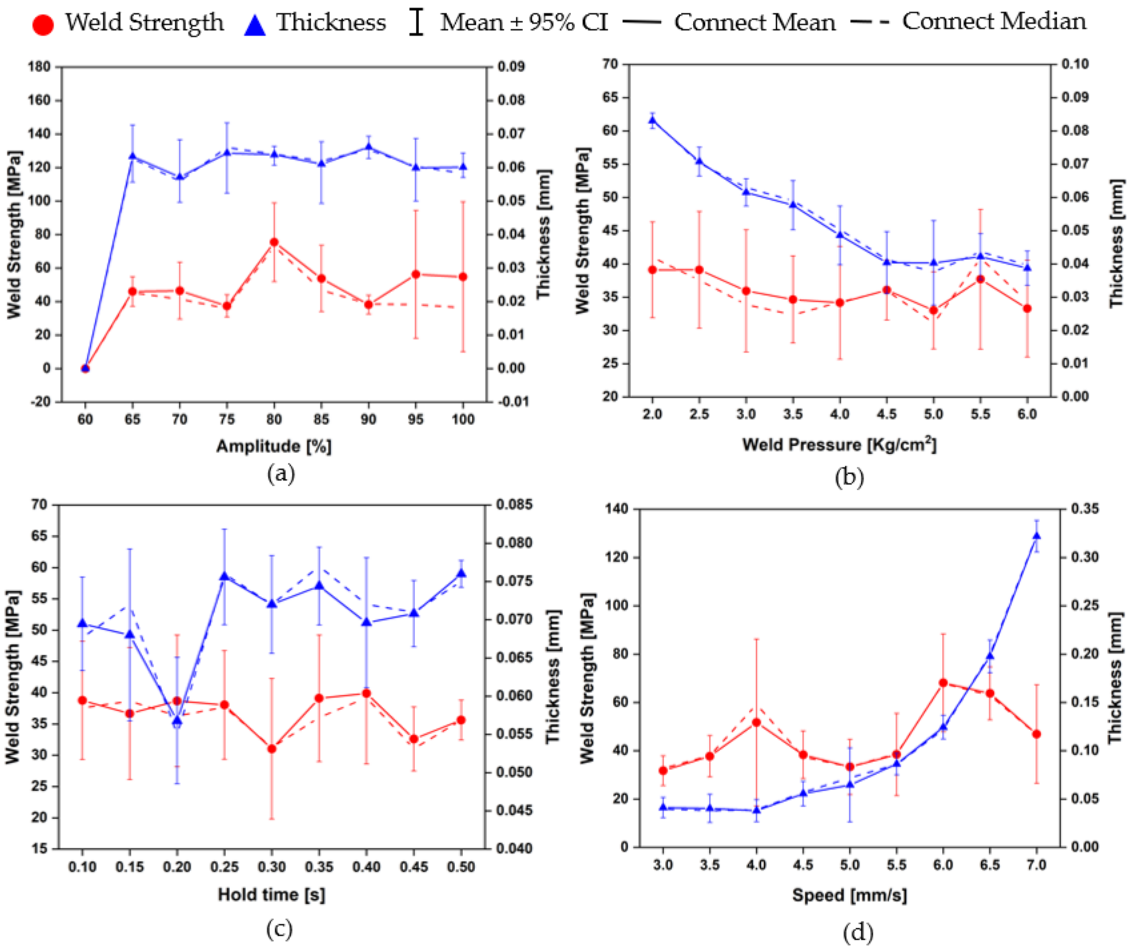

Figure 6. The result of the experiment with the levels of the variables of ultrasonic plastic welding machine for polyamide material. (**a**) amplitude; (**b**) weld pressure; (**c**) hold time; (**d**) speed.

Table 2. Factors and levels used for process.

Materials	Factors	Symbol	Units	Level 1	Level 2	Level 3
PA	Amplitude	A	%	80	85	90
	Weld pressure	P	kg/cm^2	2.0	2.5	3.0
	Hold time	T	s	0.35	0.40	0.45
	Speed	S	mm/s	5.5	6.0	6.5
PP	Amplitude	A	%	80	85	90
	Weld pressure	P	kg/cm^2	2.0	2.5	3.0
	Hold time	T	s	0.15	0.20	0.25
	Speed	S	mm/s	5.5	6.0	6.5

3.2. Polypropylene

Figure 7 shows the interval plots for the thickness and strength of polypropylene welds when the control factors were maintained at different levels. Considering the amplitude coefficient (Figure 7a), the histogram shows amplitude levels varying from 24 μm to 40 μm (60% to 100%), while the other factors were fixed (Table 1). The thickness of the weld did not change much (0.02 mm to 0.03 mm), while the strength of the weld tended to decrease at 70% (40 Mpa) and 100% (45 Mpa) and peaked at 65% (70 Mpa) and 90% (90 Mpa). Similar to the polyamide material, grade 7 with 90% margin provided the best results for the material. In terms of the weld pressure factor (Figure 7b), the welding pressure levels varied from 2.0 kg/cm^2 to 6.0 kg/cm^2. When the welding pressure increased, the strength of the weld tended to decrease, while the thickness fluctuated in the range of 0.02 mm to 0.03 mm. For this factor, when weld strength was still a priority, level 2 (2.5 kg/cm^2) provided the most optimal value. In the five samples tested at level 5, one result for the weld strength (about 80 MPa) was higher than the rest (about 25 to 30 MPa). This may be due to the fact that the mechanical properties of the plastic fibers chosen for the test were not uniform with the rest of the test pieces. This noise signal, although yielding positive results, unintentionally causes the confidence interval of the interval plot to be negative. This problem does not affect the aim of the experiment much. In order for the experimental results to be objective, this noise signal is still kept. In terms of the holding time factor (Figure 7c), the histogram shows varying hold time levels from 0.1 s to 0.5 s, while the other factors remained fixed. The welding process remained relatively satisfactory with changing the time; the strength of the weld was the best at level 4 (0.25 s), while the thickness of the welds did not differ significantly. Considering the speed factor (Figure 7d), the graph shows that the levels of the speed factor varied from 3.0 mm/s to 7.0 mm/s. Similar to the polyamide material, when the speed increased, the thickness and strength of the weld tended to increase markedly. However, if the thickness of the weld was larger, the strength of the weld decreased (grades 8 and 9). Therefore, the best result was at level 7 (6 mm/s) with an average weld strength of 100 Mpa and a thickness of 0.06 mm. In general, the strength of polypropylene welds was better than that of polyamide, but the thickness of the weld is reduced, which is due to the filament (PA) and multifilament (PP) structure. The best three levels of control factors will be selected and are shown in Table 2.

3.3. Taguchi Method

There were nine experiments used for each material type, each experiment was repeated three times to increase the reliability with four factors and three levels selected from the previous stage shown in Table 2. The PA and PP filaments will be welded on an UPWM and tested for tensile strength using a tensile test machine (TTM). Experimental results will be optimized using the Taguchi method with the larger-is-better formula (Equation (3)) [26].

$$S/N = -10ln\left[\frac{1}{x}\sum_{i=1}^{x}\left(n_i{}^{-2}\right)\right] \tag{3}$$

where x is the number of observations and n is the observed data.

Table 3 shows the tensile test results of knots when the Taguchi method was applied using the larger-the-better formula. The standard deviation of the PP knot ranged from 7.97 to 19.56; the durability of knots was greater than 60 Mpa similar to that of the PA knot. However, the difference in the durability of the PA knot was relatively small, at only 1.16, especially in experiment number 6 (A2/P3/T1/S2).

Figure 8 shows the control factors affecting the signal-to-noise ratio of PA and PP materials [27]. In particular, for the PA knot with a small difference (ranging from 36.97 to 38.01), the amplitude of the curve tended to decrease from 38.01 to 37.12, while the weld pressure factor peaked at 2 (37.98). At the same time, control factors like hold time and speed troughed at level 2 (37.08 and 37.42). Similarly, for PP knots, the difference ranged from 37.37 to 38.71, the curve tended to increase from 37.54 to 38.51 for the amplitude factor, while the weld pressure factor peaked at 2 (37.98). At the same time, control factors like hold time and speed troughed at level 2 (37.08 and 37.42).

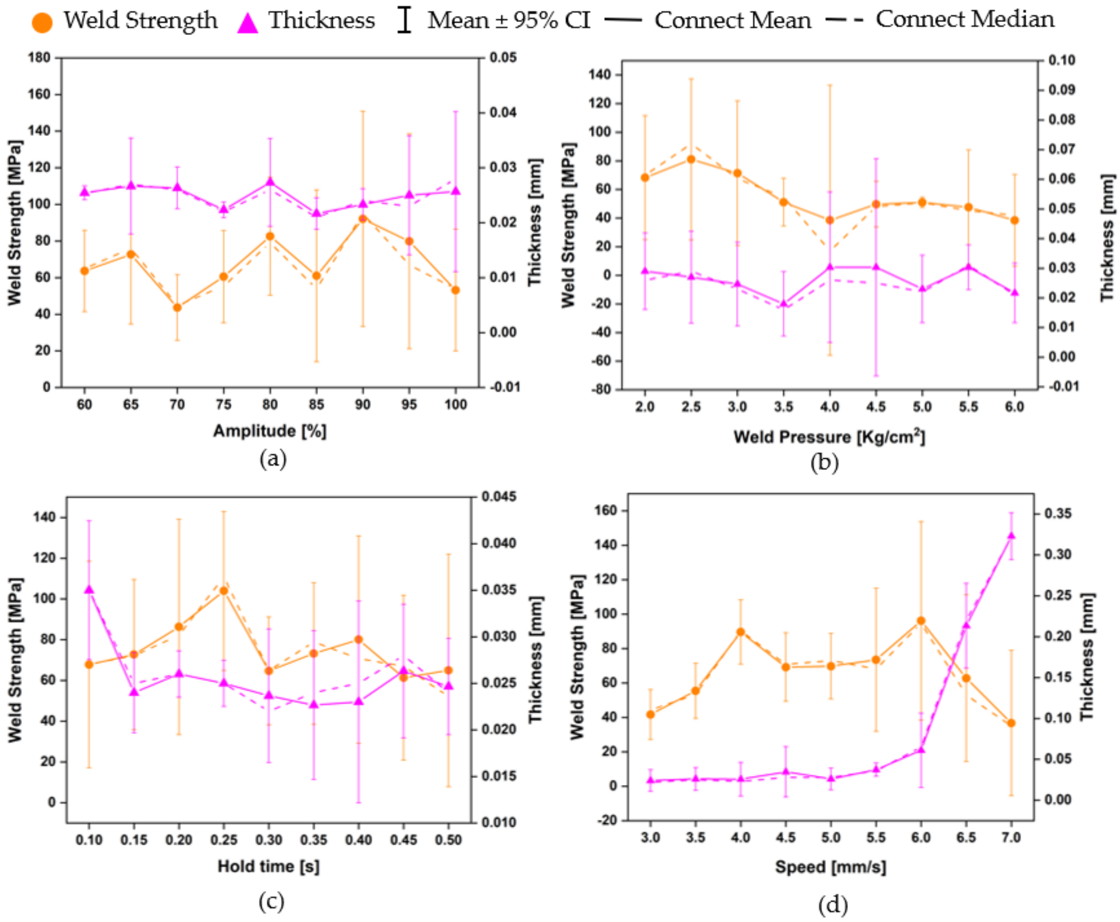

Figure 7. The result of the experiment with the levels of the variables of ultrasonic plastic welding machine for polypropylene material. (**a**) amplitude; (**b**) weld pressure; (**c**) hold time; (**d**) speed.

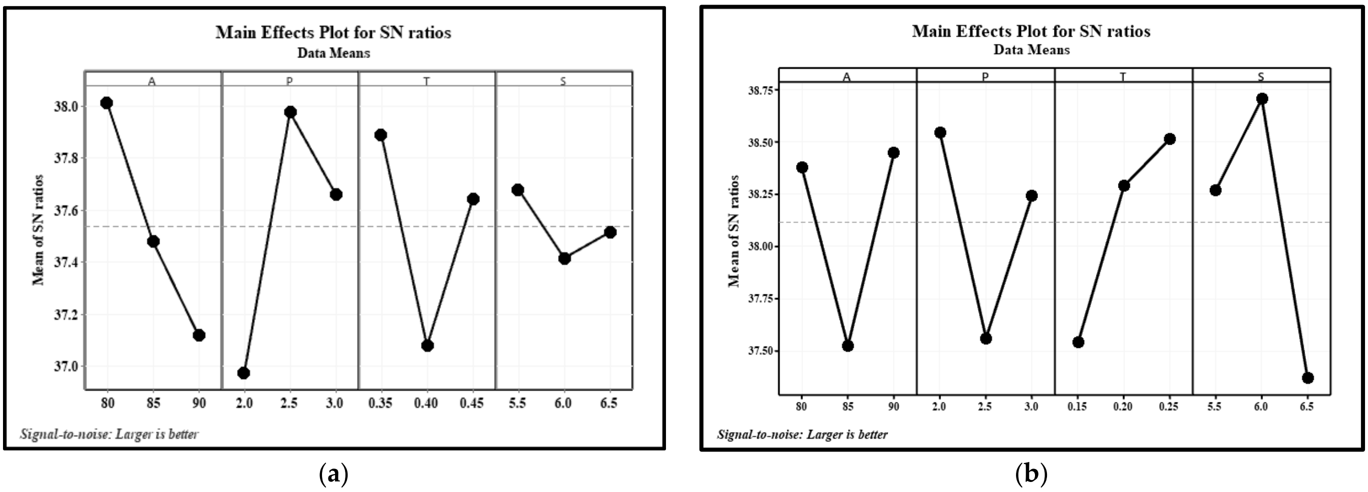

Figure 8. Process control factors affecting signal-to-noise (S/N) ratios (**a**) polyamide; (**b**) polypropylene.

Table 3. The results of tensile testing.

Experiments		Factors				Weld Strength (Mpa)			σ^2	S/N
		A	P	T	S	1	2	3		
PA	1	A1	P1	T1	S1	76.42	85.43	76.00	5.32	37.94
	2	A1	P2	T2	S2	88.15	82.93	68.11	10.39	37.87
	3	A1	P3	T3	S3	85.03	82.29	77.64	3.73	38.22
	4	A2	P1	T2	S3	73.86	63.24	63.52	6.05	36.43
	5	A2	P2	T3	S1	85.86	77.30	80.43	4.33	38.16
	6	A2	P3	T1	S2	76.65	78.74	78.57	1.16	37.83
	7	A3	P1	T3	S2	78.07	62.42	63.92	8.65	36.54
	8	A3	P2	T1	S3	72.65	78.61	85.63	6.49	37.89
	9	A3	P3	T2	S1	67.83	69.46	73.77	3.06	36.92
PP	1	A1	P1	T1	S1	107.72	68.75	85.24	19.56	38.38
	2	A1	P2	T2	S2	90.60	98.71	72.41	13.46	38.58
	3	A1	P3	T3	S3	68.60	98.35	83.72	14.87	38.15
	4	A2	P1	T2	S3	83.93	69.08	71.26	8.01	37.37
	5	A2	P2	T3	S1	72.11	70.52	85.30	8.11	37.52
	6	A2	P3	T1	S2	66.65	76.47	92.28	12.93	37.66
	7	A3	P1	T3	S2	114.63	88.40	97.43	13.32	39.86
	8	A3	P2	T1	S3	76.90	66.75	61.16	7.97	36.57
	9	A3	P3	T2	S1	104.91	81.38	83.23	13.08	38.90

Table 4 and Figure 9 show the percentage influence of control factors on the knots' durability and their ranks. In particular, for PA knots, the most influential factor was welding pressure at 41%, followed by amplitude at 34%, hold time at 24%, while the speed factor had a relatively small influence at 1%. For PP knots, the influence of factors was relatively uniform; the most influential factor being speed at 37%, followed by amplitude and weld pressure at 25% and 22%, respectively, and the last influencing factor was the hold time at 16%. The influence levels of the factors of the two materials were somewhat different; this may be because of the difference in the structure of the fibers (single for PA and group for PP) [28,29]. Specifically, the influence of the speed coefficient of PP material is higher than that of PA material. Because the thickness of the PP weld is relatively small, it affects the strength of the weld (Figure 7d). So, this factor becomes more important for PP material than for PA material.

Table 4. Response table for signal-to-noise (S/N) ratios.

Material	Polyamide (PA)				Polypropylene (PP)			
Level	A	P	T	S	A	P	T	S
1	38.01	36.97	37.89	37.68	38.38	38.54	37.54	38.27
2	37.48	37.98	37.08	37.42	37.52	37.56	38.29	38.71
3	37.12	37.66	37.64	37.52	38.45	38.24	38.51	37.37
Delta	0.89	1.00	0.81	0.26	0.92	0.98	0.98	1.34
Rank	2	1	3	4	4	2	3	1

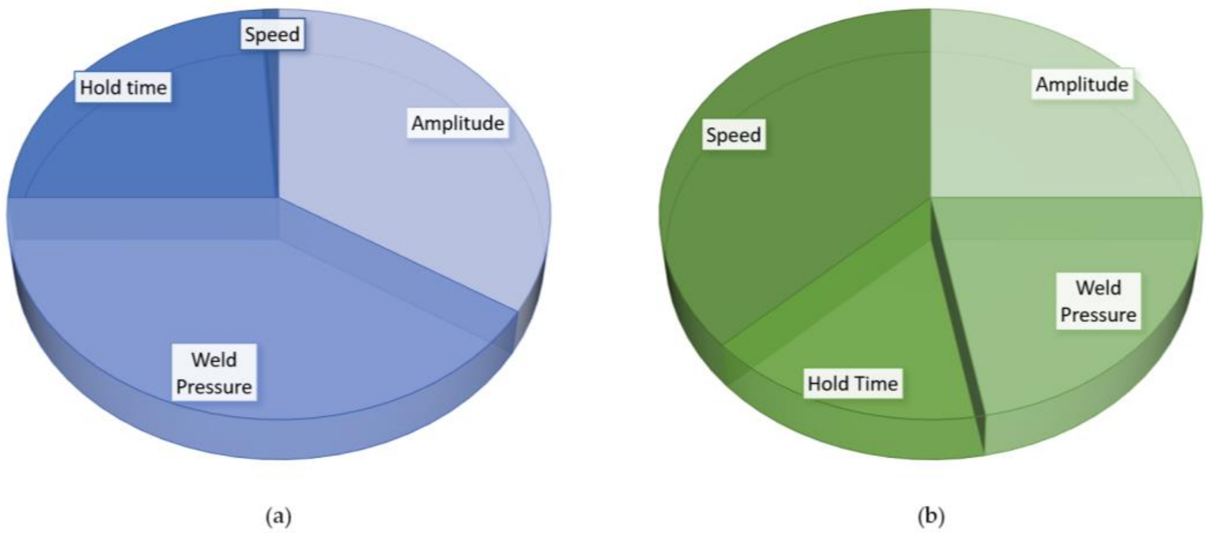

Figure 9. Percent influence of factors (**a**) polyamide; (**b**) polypropylene.

3.4. Confirmation of the Experiment

Then, the results were confirmed by applying the Taguchi method. The optimized parameter set for the PA and PP materials on the UPWM was compared with three sets of random parameters for the tensile strength shown in Table 5. After being optimized, the parameter set exhibited greater durability than the remaining parameter sets. In addition, the difference in the test samples was also relatively small, with an average value of 85.5 Mpa for the PA knot and 89.3 Mpa for the PP knot, proving the stability of the parameter set after being optimized using the Taguchi method. Figure 10 shows the interval plot of the weld strength pre- and post-optimization.

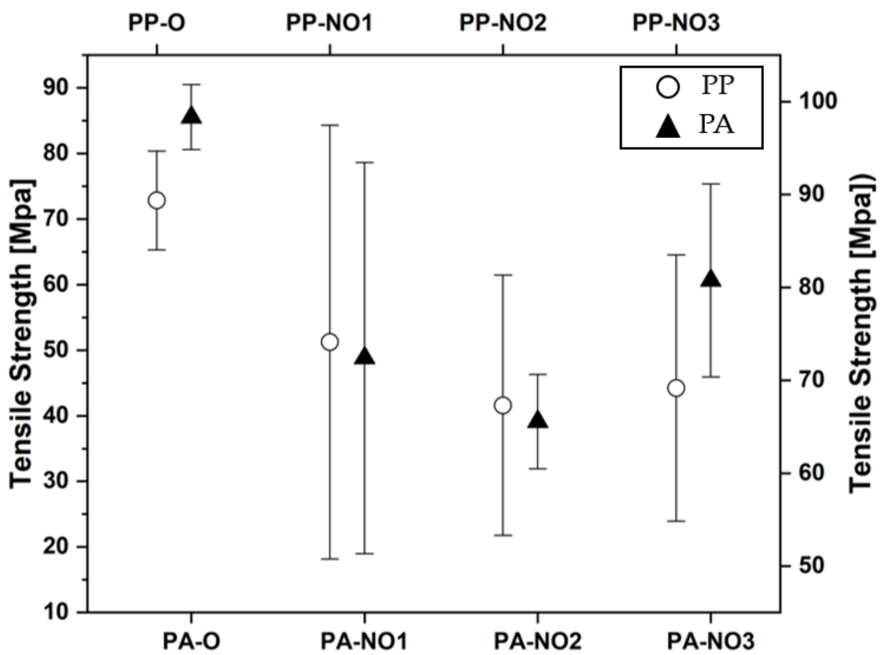

Figure 10. The results of tensile strength values of the confirmation experiment.

Table 5. The specification used to confirm the research experiment.

Material	Specification	Factors				Tensile Strength (Mpa)					
		A	P	T	S	1	2	3	4	5	Mean
PA	Optimized	80	2.5	0.35	5.5	80.7	88.6	82.4	90.1	85.8	85.5
	None optimized 1	85	3.0	0.3	5.0	41.6	36.5	44.2	90.8	30.9	48.8
	None optimized 2	80	2.0	0.3	5.0	44.4	30.12	36.8	41.0	43.2	39.1
	None optimized 3	80	3.0	0.3	6.0	76.3	45.0	66.9	54.9	60.1	60.6
PP	Optimized	90	2.0	0.25	6.0	89.4	84.4	95.6	86.6	90.7	89.3
	None optimized 1	95	3.0	0.3	5.0	107.1	65.5	66.9	70.6	60.4	74.1
	None optimized 2	80	2.0	0.3	5.0	84.9	69.9	60.7	65.8	55.2	67.3
	None optimized 3	80	3.0	0.35	5.0	78.9	83.5	57.3	60.2	65.8	69.1

4. Conclusions

For polyamide and polypropylene mesh weaving developed using the UPWM, the control factors (amplitude, weld pressure, hold time, and speed) of the UPWM were optimized via the Taguchi method. The influence levels of the factors of the two materials were somewhat different; this may be because of the difference in the structure of the fibers. The following are the findings of this study:

- The knots made from PA filament after welding via the UPWM have stable strength at 75% compared to the original PA filament, with the following parameters after optimization: an amplitude of 32 μm (34%), a welding pressure of 2.5 kg/cm^2 (41%), a hold time of 0.35 s (24%), and a speed of 5.5 mm/s (1%).
- The knots made of PP filament had relatively stable strength with the following parameters after optimization: an amplitude of 36 μm (25%), a welding pressure of 2.0 kg/cm^2 (22%), a hold time of 0.25s (16%), and a speed of 6.0 mm/s (37%).
- In addition, the difference in the strength of the knots after optimization was significantly improved. However, the thickness of the knots after UW application was relatively small compared to that of the original rope, leading to the low strength of the knots. During the experiment, changing the speed increased the thickness, but reduced the adhesion of the weld. Therefore, it was necessary to reinforce typical materials such as thin films at the location of the knots.
- This research has important implications for the application of UPWM in the manufacture of trawl nets or similar polymer materials. It allows for the selection of welding parameters that are simpler, more cost-effective, systematic, and fast.

Author Contributions: Writing—original draft preparation, N.-D.N.; writing—review and editing, N.-D.N. and S.-C.H. All authors have read and agreed to the published version of the manuscript.

Funding: The authors recognize and thank the National Science and Technology Council of the Republic of China for its partial financial support of this work under Contract Number NSTC 112-2221-E-992-040.

Institutional Review Board Statement: Not applicable.

Informed Consent Statement: Not applicable.

Data Availability Statement: Data are contained within the article.

Conflicts of Interest: The authors declare no conflict of interest.

References

1. Suzuki, K.; Takagi, T.; Shimizu, T.; Hiraishi, T.; Yamamoto, K.; Nashimoto, K. Validity and visualization of a numerical model used to determine dynamic configurations of fishing nets. *Fish. Sci.* **2003**, *69*, 695–705. [CrossRef]
2. de Dios Rivera, J.; Lopez-Garcia, D. Mechanical characteristics of Raschel mesh and their application to the design of large fog collectors. *Atmos. Res.* **2015**, *151*, 250–258. [CrossRef]
3. Beveridge, M. *Cage Aquaculture*, 3rd ed.; Blackwell Publishing: Hoboken, NJ, USA, 2004.
4. Chen, H.; Christensen, E.D. Development of a numerical model for fluid-structure interaction analysis of flow through and around an aquaculture net cage. *Ocean Eng.* **2017**, *142*, 597–615. [CrossRef]
5. Su, B.; Kelasidi, E.; Frank, K.; Haugen, J.; Føre, M.; Pedersen, M.O. An integrated approach for monitoring structural deformation of aquaculture net cages. *Ocean Eng.* **2020**, *219*, 108424. [CrossRef]
6. Baranowski, P.; Małachowski, J.; Niezgoda, T.; Mazurkewicz, Ł. Dynamic behaviour of Various Fibre Systems During Impact Interaction—Numerical Approach. *Fibres Text. East. Eur.* **2015**, *23*, 72–82. [CrossRef]
7. Jensen, Ø.; Dempster, T.; Thorstad, E.; Uglem, I.; Fredheim, A. Escapes of fishes from Norwegian sea-cage aquaculture: Causes, consequences and prevention. *Aquac. Environ. Interact.* **2010**, *1*, 71–83. [CrossRef]
8. Tsujino, J.; Hongoh, M.; Tanaka, R.; Onoguchi, R.; Ueoka, T. Ultrasonic plastic welding using fundamental and higher resonance frequencies. *Ultrasonics* **2002**, *40*, 375–378. [CrossRef]
9. Kuo, C.-C.; Tsai, Q.-Z.; Li, D.-Y.; Lin, Y.-X.; Chen, W.-X. Optimization of Ultrasonic Welding Process Parameters to Enhance Weld Strength of 3C Power Cases Using a Design of Experiments Approach. *Polymers* **2022**, *14*, 2388. [CrossRef]
10. Mahmoudian, M.; Marjani, A.P.; Hasanzadeh, R.; Moradian, M.; Shishavan, S.M. Optimization of mechanical properties of in situ polymerized poly(methyl methacrylate)/alumina nanoparticles nanocomposites using Taguchi approach. *Polym. Bull.* **2019**, *77*, 2837–2854. [CrossRef]
11. Costa, D.M.D.; Paula, T.I.; Silva, P.A.P.; Paiva, A.P. Normal boundary intersection method based on principal components and Taguchi's signal-to-noise ratio applied to the multiobjective optimization of 12L14 free machining steel turning process. *Int. J. Adv. Manuf. Technol.* **2016**, *87*, 825–834. [CrossRef]
12. Jian, B.-L.; Wang, C.-C.; Yau, H.-T.; Wu, L.-W.; Tian, A.-H. Optimization of Lathe Cutting Parameters Using Taguchi Method and Grey Relational Analysis. *Sens. Mater.* **2020**, *32*, 843–858. [CrossRef]
13. Danh, N.N.; Son, T.D. The solution of taking net-wrapper automatically by using principle of suction fan. *J. Austrian Soc. Agric. Econ.* **2021**, *17*, 807–816.
14. Liu, Z.; Li, Y.; Liu, Z.; Yang, Y.; Li, Y.; Luo, Z. Ultrasonic Welding of Metal to Fiber-Reinforced Thermoplastic Composites: A Review. *J. Manuf. Process.* **2023**, *85*, 702–712. [CrossRef]
15. Mercer, W.B.; Hall, A.D. The Experimental Error of Field Trials. *J. Agric. Sci.* **1911**, *4*, 107–132. [CrossRef]
16. Robert Wayne Atkins. Gill Nets | Robert Wayne Atkins, P.E. grandpappy.org. 2009. Available online: https://grandpappy.org/wgillnet.htm (accessed on 25 April 2023).
17. Briassoulis, D.; Mistriotis, A.; Eleftherakis, D. Mechanical behaviour and properties of agricultural nets. Part II: Analysis of the performance of the main categories of agricultural nets. *Polym. Test.* **2007**, *26*, 970–984. [CrossRef]
18. Madueke, C.I.; Mbah, O.M.; Umunakwe, R. A review on the limitations of natural fibres and natural fibre composites with emphasis on tensile strength using coir as a case study. *Polym. Bull.* **2022**, *80*, 3489–3506. [CrossRef]
19. Shen, D.; Liu, C.; Luo, Y.; Shao, H.; Zhou, X.; Bai, S. Early-Age Autogenous Shrinkage, Tensile Creep, and Restrained Cracking Behavior of Ultra-High-Performance Concrete Incorporating Polypropylene Fibers. *Cem. Concr. Compos.* **2023**, *138*, 104948. [CrossRef]
20. Bernasconi, A.; Davoli, P.; Basile, A.; Filippi, A. Effect of fibre orientation on the fatigue behaviour of a short glass fibre reinforced polyamide-6. *Int. J. Fatigue* **2007**, *29*, 199–208. [CrossRef]
21. Montgomery-Liljeroth, E.; Schievano, S.; Burriesci, G. Elastic properties of 2D auxetic honeycomb structures—A review. *Appl. Mater. Today* **2023**, *30*, 101722. [CrossRef]
22. Pham, D.B.; Huang, S.-C. A novel bio-inspired hierarchical tetrachiral structure that enhances energy absorption capacity. *J. Mech. Sci. Technol.* **2023**, *37*, 3229–3237. [CrossRef]
23. Wang, S.; Lin, S. Optimization on Ultrasonic Plastic Welding Systems Based on Two-Dimensional Phononic Crystal. *Ultrasonics* **2019**, *99*, 105954. [CrossRef]
24. Hussen, M.S.; Kyosev, Y.K.; Pietsch, K.; Rothe, S.; Kabish, A.K. Effect of ultrasonic welding process parameters on peel strength of membranes for tents. *J. Eng. Fibers Fabr.* **2022**, *17*, 1–19. [CrossRef]
25. Khan, M.I.; Umair, M.; Hussain, R.; Karahan, M.; Nawab, Y. Investigation of impact properties of para-aramid composites made with a thermoplastic-thermoset blend. *J. Thermoplast. Compos. Mater.* **2021**, *36*, 866. [CrossRef]
26. Nguyen, N.-D.; Huang, S.-C. Trawl Grid Structure Design and Analysis Using the Finite Element Method. *Appl. Sci.* **2023**, *13*, 7536. [CrossRef]
27. Hiwa, B.; Ahmed, Y.M.; Rostam, S. Evaluation of tensile properties of Meriz fiber reinforced epoxy composites using Taguchi method. *Results Eng.* **2023**, *18*, 101037. [CrossRef]

28. Pejkowski, Ł.; Seyda, J.; Nowicki, K.; Mrozik, D. Mechanical performance of non-reinforced, carbon fiber reinforced and glass bubbles reinforced 3D printed PA12 polyamide. *Polym. Test.* **2023**, *118*, 107891. [CrossRef]
29. Almeshari, B.; Junaedi, H.; Baig, M.; Almajid, A. Development of 3D printing short carbon fiber reinforced polypropylene composite filaments. *J. Mater. Res. Technol.* **2023**, *24*, 16–26. [CrossRef]